Dynamic Analysis with Fibre Optic Sensors for Structural Health Monitoring

Antonio Paolozzi, Paolo Gasbarri
University of Rome La Sapienza, Aerospace and Astronautic Department
Via Eudossiana, 18
00184 Rome
ITALY

antonio.paolozzi@uniroma1.it

ABSTRACT

Structural Health Monitoring (SHM) is a new frontier of non destructing testing. Often SHM is associated with fibre optic sensors whose signals can be used to identify the structure and consequently its damage. Two ways of performing such an identification is either through the modal properties or through a direct use of time domain responses. Time domain techniques allows through inverse problem procedures to retrieve mass and stiffness matrices. The most common approach followed to retrieve dynamic parameters of a structure is called experimental modal analysis. This approach determines modal parameters (i.e. mode shapes, natural frequencies and modal damping) of the structure through the responses induced by known and sometimes unknown excitations (output only techniques).Modal parameters not only are useful for structural identifications but also to determine the resonances of the structures so that design changes can be performed if excitation frequencies are too close to ones of those resonances. So one can determine the damage, looking directly at the modal parameter variation or at changes in the structural matrices that can be derived, at least in principle, from the modal model. In the paper both modal analysis and time domain techniques will be described: modal appropriation technique with Electronic Speckle Pattern Interferometry (ESPI), classical broad band, broad band and stepped sign with the use of fibre optic sensors and inverse problems for time domain responses. In the paper numerical results relevant to damage identification in time domain will be presented, but particular emphasis will be given to the use of fibre optic sensors (specifically the Fibre Bragg Gratings or FBGs and sensorless fibre in a Michelson interferometer). Since in Structural Health Monitoring embedded sensors are usually considered, in the paper some embedding procedures for metallic materials by casting, as well as for composite materials by the hand lay-up and vacuum bagging technique will also be shown. Finally a case in which the optical fibre has been attached in the same way as a conventional strain gage will be shown. In all cases experimental results relevant to dynamic tests will be presented. It is worth noting that differently from the accelerometers, FBGs work very well in dynamics as well as in statics.

1 INTRODUCTION

SHM can be associated to vibration measurements. In fact structural response changes are related to damage. These responses can be worked out directly in the time domain or also in the frequency domain. In this last case the reduction of vibration data can be performed by using a well known reduction technique called experimental modal analysis.

Optical fibres as a damage monitoring system on a structure have been used for the first time in [1]. In the eighties fibre optic sensors were not well developed and therefore plain optical fibres were used. With that limitation only the failure of an optical fibre could be associated to structural damage.

Paolozzi, A.; Gasbarri, P. (2006) Dynamic Analysis with Fibre Optic Sensors for Structural Health Monitoring. In *Multifunctional Structures / Integration of Sensors and Antennas* (pp. 9-1 – 9-24). Meeting Proceedings RTO-MP-AVT-141, Paper 9. Neuilly-sur-Seine, France: RTO. Available from: http://www.rto.nato.int/abstracts.asp.

Nowadays, some devices developed for the telecommunication market, can be used as very small and integrated sensing devices. Particular relevance for structural application is given by the Fibre Bragg Gratings (FBGs) that are basically strain optic sensors but offer several advantages over the conventional ones. FBGs can be multiplexed along the same fibre. In fact usually the sensors are interrogated by injecting into the fibre a broad band infrared signal 40 nm wide. Each sensor, reflects a specific wavelength, called Bragg wavelength, that carries the strain information. Also, due to the small diameter of the optical fibres (conventional from 150 to 250 μm including the coating; special with diameter of about 40 μm) they can be easily embedded into composite materials [2-7]. It has been proven in several papers also the possibility of embedding optical fibres into metallic materials [8-12]. These sensors can be used not only for crcak detection [13-14] but also for impact assessment [15] and for position monitoring [16,17]. One way of performing SHM is through modal analysis. In Ref. [6] natural frequencies have been obtained using a sensorless optical fibre embedded into a Glass Fibre Reinforced Plastics (GFRP) and inserted into an interferometer. In Refs. [18,19] a similar procedure was follow on a zinc-aluminium alloy slender bar. However this way only the total strain integrated over the embedded length could be found while to retrieve all modal parameters (mode shapes, and modal damping besides natural frequencies), point responses are required. We have obtained the first dynamic point strain measurement from embedded FBGs in Refs. [20-22]. In particular in Ref. [22] the Strain Frequency Response Functions (SFRFs) of a Carbon Fibre Reinforced Plastic (CFRP) beam with an embedded FBG have been obtained while in Ref. [23] the first and second strain mode shape of the same bar have been retrieved from the SFRF. From now on the mode shapes retrieved from SFRF, will be referred to as strain mode shapes. In this paper some of the results referenced above will be briefly recalled along with some newer applications with more complex structures where also an FBG interrogation system with high acquisition rate has been used. This last instrument will allow the retrieval of strain mode shapes other than the first one. The SFRFs are similar to the conventional FRFs obtained by impact hammer and accelerometers. For the retrieval of strain modes, the same rules and algorithms used for the conventional mode shapes are followed.

2 EXPERIMENTAL MODAL ANALYSIS

In this section we will review some work we performed in this field starting with a relatively new technique in the class of modal appropriation techniques. Then we will move to broad band techniques with a special attention devoted to the case in which the structural response is given by a fibre optic or by Fibre Bragg Gratings. Experimental modal analysis seeks modal parameters and possibly mass and stiffness matrices through the acquisition of responses induced by known (such as impulse and random) and sometimes unknown excitations. Furthermore the knowledge of modal parameters is important because even intuitively one knows that sinusoidal excitation may be very dangerous if its frequency is close to one of the natural frequencies of the structure. Furthermore from the modal model it is in principle possible to determine the so-called spatial model of the structure, i.e. the stiffness, mass and damping matrices.

There are basically two ways for performing experimental modal analysis: (i) modal appropriation technique,(ii) broad band technique. In the modal appropriation technique, the structure is forced to vibrate according to one of its natural modes. Theoretically in the broad band technique all the modes are excited at the same time.

2.1 Modal Appropriation Technique

Holographic interferometry [24-27] or its electronic version, known as the Electronic Speckle Pattern Interferometry (ESPI) [27-30], can be both considered modal appropriations techniques. In this case full field mode shapes can be obtained in the form of fringe patterns. It is also possible to obtain a 3D representation of the mode shapes by developing, for special cases, proper software such as the one shown

in Ref. [31] or by using more general purpose commercial codes. The excitation (sinusoidal or stepped sine) is usually provided either with a loudspeaker (mainly used for light, not massive structures) or with a piezoelectric patch attached in a proper location on the structure. Sometimes, thanks to the sensitivity of the method, the exciter can be attached on the constrained part of the structure. Elastic waves propagates through the test item and vibration modes can be detected. These techniques actually measure the stationary patterns of vibration that, in general, can be obtained with a combination of two consecutive modes. In Ref. [32] a technique is proposed based on Modal Assurance Criterion (MAC) for recognising the modes contributing to the stationary vibration patterns. In an example taken from Ref. [30] we report the scheme of the experimental set-up (Fig. 1). A photograph along with a drawing of the test item and a detail of the clamped end is shown in Fig. 2. The test item is UNISAT 1, a microsatellite built at our department by the "Gruppo di Astrodinamica Università degli Studi la Sapienza" (GAUSS) and launched on the 26th of September 2000, (UNISAT 2 has been launched on the 20th of December 2002 while UNISAT 3 was launched on the 29th of June 2004). In Fig. 1 a laser beam is divided by the beam splitter into the object and reference beam. The optical path of this last one is controlled by a piezo-controlled mirror. The object beam illuminates the structure of the microsatellite. The two beams recombine at the CCD of the TV camera providing images such as those reported in Fig. 3. The two computers have been used to monitor the excitation and for grabbing the images. As mentioned, this type of excitation is conceptually not very close to the ideal excitation required to consider the method a perfect modal appropriation technique. In fact neighbouring modes happens to be excited, even if at very low level. That can be seen in Fig. 3 where the actual modes are detected at 1800 Hz and 1860 Hz, while all the other stationary patterns are a combination of two modes.

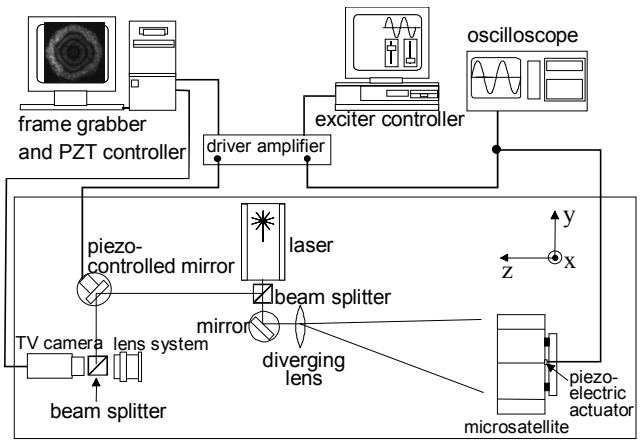

Figure 1: Experimental set-up for ESPI.

2.2 Broad Band Technique

These methods are based on the acquisition of the transfer functions. The transfer function transforms the excitation input in the response structural output (e.g. force as input and acceleration as output) working in the frequency domain. The transfer function are organised in the transfer matrix. One row (containing the transfer functions between a single input point and all the output points), or one column (containing the transfer functions between all the input point and a single output point) is sufficient to obtain the complete matrix (matrix is of rank 1) and consequently, by employing various fitting techniques, it is possible to obtain the structural vibration modes (frequency, damping and shapes). The acquisition of more rows or columns of the transfer matrix will increase the confidence in the performed analysis.

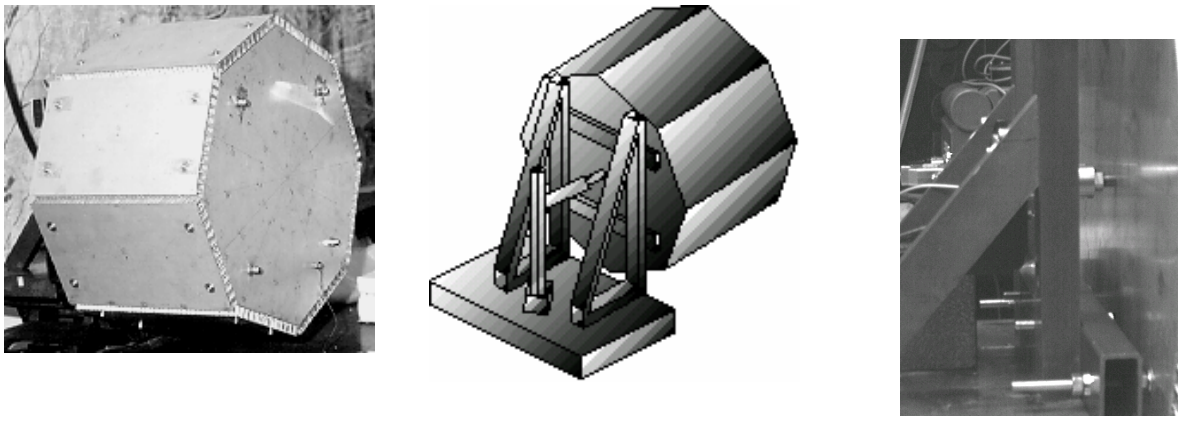

Figure 2: View and drawing of constrained satellite and detail of piezoelectric actuator used for excitation.

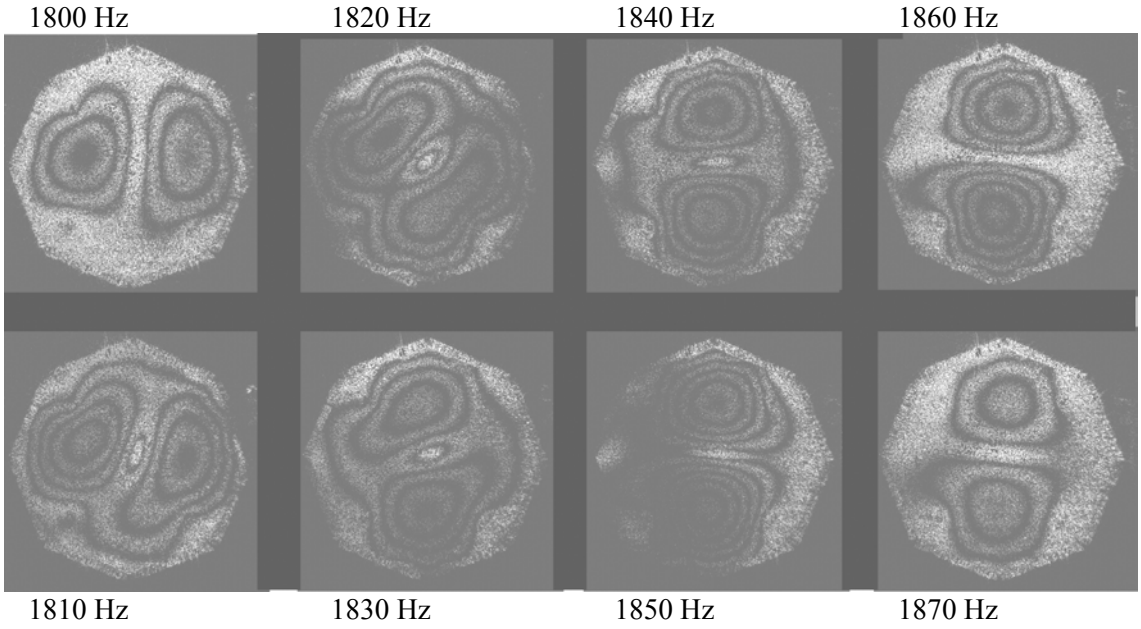

Figure 3: Experimental ESPI fringe patterns of top surface of UNISAT satellite.

Such methodologies are now widely employed due to the large selection of Fast Fourier Transform (FFT) analyser now available also on PC-cards. For this class of methods just one single exciter, working at broadband, is enough to acquire the FFT. The possibility to excite the structure on more frequencies at the same time allows the simultaneous acquisitions of modal parameters of all modes in the interested band independently from the excitation signal. The excitation is generally random or impulsive [33,34] that both have energy spectral density nearly constant in the frequency range of interest. FFT analysers are relatively easy to use and fast, and allow to obtain statistical estimates of transfer functions. Extraction of modal parameters is performed using one of the many fitting methods available either in the frequency or in the time domain. They can be single (SDOF) or multi degrees of freedom (MDOF) methods.

By using multiple excitations it is possible to improve parameter estimates. In fact the use of more exciters placed in suitable location in the structure allows a more uniform distribution of energy using lower levels of excitation. That means local non-linearities are not excited. This approach has been applied to the

modal analysis of the Space Shuttle Enterprise [35]. A particular multi input excitation is the two input excitation used in the modal analysis of the Boeing 757 and Boeing 767 [36]. Such an excitation allows to obtain independent modal vector estimates and through linear combination, helps to separate modes. In particular for symmetric excitation, such a technique, with simple summation and subtraction of the columns of the Transfer Matrix, points out symmetrical and anti-symmetrical modes.

3 STRUCTURAL HEALTH MONITORING WITH OPTICAL FIBRES AND MODAL ANALYSIS

In the broadband test Frequency Response Functions (FRFs) are acquired and used to determine the modal parameters. Usually responses are obtained from accelerometers. There is however an alternative way of obtaining dynamic responses using strain gages. In Ref. [37] is reported the theoretical basis of this approach.

By Structural Health Monitoring (SHM) one means a system with embedded or surfaces attached sensors that provides information on the state of the structure in analogy with nervous system of living beings The advantage of SHM is that a limited amount of manpower and resources is required for maintenance. In a complex system such as the NASA Space Transportation System (STS), (well known as Space Shuttle) hundreds of people and several weeks are required to refurbish and check the vehicle. With a SHM system many of those operations will be automated providing a less expensive and possibly more reliable approach. Of course the technological challenges are very demanding and a lot of money has to be invested in research and prototype development. Many researchers are working today in this field and specialized conferences (such as the International Workshop on Structural Health Monitoring and the European Workshop on Structural Health Monitoring) and journals are devoted to the topic. Results presented in many papers are very promising. In the following we will present our best results obtained recently in this direction.

As mentioned experimental modal analysis may be used as a tool for understanding the health state of the structures through the modal parameter variation. In Refs. [38-41] for instance we have used conventional instrumentation (accelerometers, impact hammer, FFT analyser) to study the effect of damages on modal parameters. In the following instead we will show an original approach that relies on optical fibres to achieve such a goal.

There are several types of fibre optic sensors, here we will limit our analysis at the Fibre Bragg Grating (FBG) sensors and to sensorless optical fibres. FBGs are basically optical strain gages in that they provide strain measurements along the fibre direction. They are typically characterized by a sinusoidal fluctuation of the index of refraction of the fibre core. The length of the sensor is usually 1 cm while the wavelength Λ of the sinusoidal fluctuation is typically 0.5 μm. Differently from the conventional strain gages they can be multiplexed in the same fibre reducing consequently the harness of the installation. The measurement consists in an optical wavelength shift of the Bragg wavelength λ_B induced by strain. The Bragg wavelength is an intrinsic characteristics of the FBG since it is determined by the following relation:

$$\lambda_B = 2n\Lambda$$

where Λ, as mentioned, is the pitch of the variation of the index of refraction while n is the index of refraction of the fibre core. Now we will describe some applications where the fibre has been embedded into metallic materials by casting, as well as into composite materials by the hand lay-up and vacuum bag technique. Finally a case in which the optical fibre has been attached in much the same way as a conventional strain gage is shown. In all cases only some results relevant to dynamic tests will be presented. It is worth noting that in contrast to the accelerometers, FBGs work very well in dynamics as well as in statics.

3.1 Dynamic Test with an Embedded Optical Fibre in a Metallic Beam

The possibility of embedding optical fibres into metals or ceramics has not been explored by many people because the difficulties are much greater than in polymeric composite materials. The high temperatures involved in a casting process, or the high mechanical stresses involved during the lamination makes the embedding procedure difficult. In Ref. [10] the first attempt to embed an optical fibre into an aluminium alloy was successful and encouraged us to try to perform static [11,12] and vibration [18-21] tests using sensorless optical fibres. In particular in Ref. [19] it was performed a broad band test in which we were able to acquire a Strain Frequency Response Function (SFRF) instead of a conventional Frequency Response Function (FRF). In this case the strain was integrated over the whole length of the embedded fibres. In Fig. 4 is reported a sketch of the experimental set-up. The laser beam is splitted into two coherent beams and launched into the two optical fibres. One is the reference optical fibre and the other one is the embedded optical fibre. Whenever the beam stretches, the optical path changes.

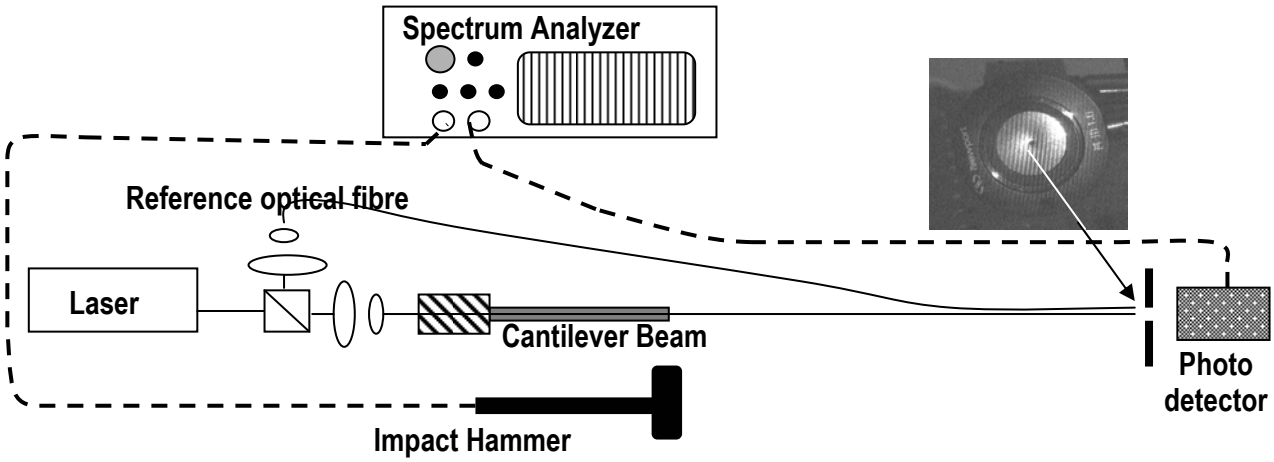

Figure 4: Experimental set-up of the metallic beam with embedded optical fiber.

As a consequence the fringes will move and the photodetector will detect a modulation on the light intensity. That signal, transformed into the frequency domain, will give information on the resonant frequencies of the bar. In Fig. 5 it is reported the Power Spectral Density (PSD) of the signal obtained by hitting the bar with the instrumented impact hammer. As one can see from the spectrum the first resonant frequency of the cantilevered bar is 100.25 Hz. Clearly this frequency can be used as a first indication of the state of health of the component. The whole set-up is an example of a simple structural health monitoring system. The limitation of this system is that only natural frequencies can be retrieved. In order to obtain the mode shapes local strain measurements are needed. In Ref. [20] the embedding of an FBG has been successfully obtained. However due to the high first resonant frequency of the Zn-Al bar, only static tests and low frequency forced sinusoidal vibration tests have been conducted using the embedded FBG and the commercial fibre optic interrogation system. An experimental modal analysis for that specimen is foreseen in the near future after the procurement of a high frequency FBG interrogation system. A complete experimental modal analysis has been instead conducted successfully on a composite specimen and on a star tracker prototype as will be described in the next section.

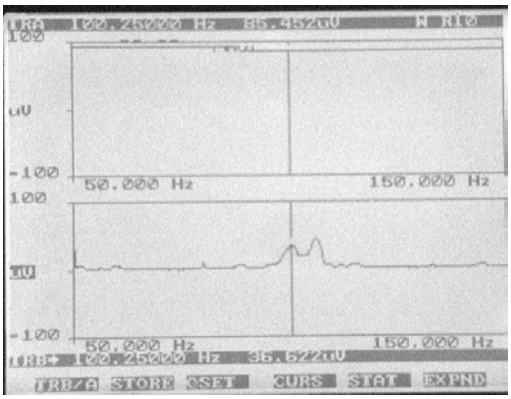

Figure 5: Experimental results: PSD obtained from the test of Fig. 4 impact force (top) and of photo-detector (bottom).

3.2 Modal Analysis with Embedded Optical Fibres in Composite Structure

The process of embedding fibre optic sensors into composite material is almost a standard procedure [2-7]. The main difficulty one encounters is the possibility that the fibre breaks at the ingress and/or egress from the component.

3.2.1 Beam Structure

In the case of the beam structure the ingress-egress problem of the fibres from the component was solved by using a Teflon or kapton ribbon as shown in Fig. 6. A more attractive approach is to embed the connectors (this approach has been followed in the next section). Unfortunately the ones used in telecommunication are too big for the usual thickness of composite laminates. However miniaturization of connectors is underway and that is certainly an important step towards industrial application of this technology. In Fig. 7 is reported a composite bar during the lamination. Two optical fibres are visible while handling them.

The most convenient location along the thickness for an FBG sensor is away from the neutral axis. This choice will allow to sense bending of the structure. By putting two sensors in opposite position with respect to the neutral axis it will be possible to separate bending from tension. In analogy with the conventional experimental modal analysis with accelerometer, one retrieves the (SFRF) first [22] and then the modal parameters. In particular from SFRF one obtains strain modes instead of the displacement modes. In Ref. [23] for the first time (to our knowledge nothing similar can be found in the literature) we have obtained a strain mode (Fig. 8) from the SFRF obtained using one FBG of the bar shown in Fig. 7. The results were completely compatible with those obtained with an accelerometer.

Figure 6: Teflon ribbon protecting the egress of optical fibres from a CFRP laminate.

Figure 7: Handling of the two optical before the embedding process.

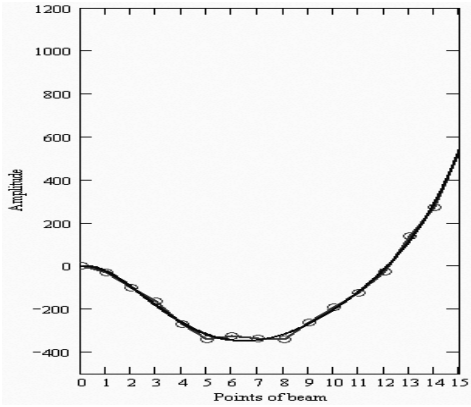

Figure 8: Second mode shape obtained by the FBG. Circles (exp. data); solid line (fit of exp. data).

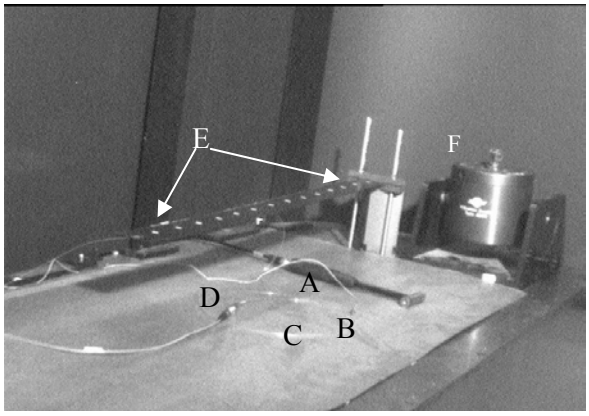

Figure 9: Views of experimental set-up. A: impact hammer; B: accelerometer; C: optical fibre; D: optical fibre connector; E: experimental grid F: shaker.

The test has been performed with a commercial FBG interrogation system (see Fig. 9 for test set-up). The interrogation system is a unit that is capable of reading with an extreme accuracy the wavelength shift of λ_B. As a consequence the strain resolution is lower than 1 με. The commercial unit had the limit of about 50 readings per second. That means the maximum frequency of the mode shape one can capture is about 20 Hz (Shannon Theorem). For that reason the bar of Fig. 7 was designed in such a way to have the first two resonant frequencies below 20 Hz.

3.2.2 Wing Structure of an Airplane Model

Four Fibre Bragg Gratings (FBGs) have been embedded in one wing (1.3 m long) of a model of an unmanned aircraft (Fig. 10). The sensors have provided real time strain measurements. Each wing of the aircraft has been manufactured as a sandwich with polystyrene core and one ply of Glass Fabric (GF) (0/90) characterized by a density of 80 g/m^2. An epoxy resin with the relevant curing agent has been applied manually. The two parts of the polystyrene core have been cut using a hot wire machine. The first

layer of GF has been put on the two separate sections of the core. Then the I section spar of the wing was prepared connecting two C section of GF (0/90) and two slender plates of Carbon Fabric (CF) on each side characterized by a density of 200 g/m^2 (see Fig. 11). Also here the epoxy resin and the curing agent has been applied manually with a proper tool. Four fibres (two on the top and two on the bottom of the I spar) with one FBG each were positioned on the I spar. Finally one layer of GF with epoxy resin has been used to cover the whole assembled wing. Due to the presence of the polystyrene it was not possible to cure the composite into an autoclave. Therefore external loads have been applied on the wing surface and 24 hours were required to completely cure the resin at room temperature. In Fig. 12 is reported a picture of the wing mounted on a fixture for dynamic test.

Figure 10: Photograph of the aircraft model.

The Glass Fibre Reinforced Plastic (GFRP) is transparent and consequently allows to see the spar as well as the polystyrene body of the wing. The white dots on the spar are removable tags used to label the experimental grid used in the subsequent modal analysis test. In Fig. 11 two fibres are visible (see the two lines on top of the CFRP rectangular slender plate). The other two sensors have been embedded symmetrically with respect to the wing body and are not visible in the picture. In Figs. 13 and 14 are reported the finite element model of the wing and its second natural mode. The wing has been clamped in one end (see detail in Fig. 12b). The constraint interface, clearly visible in Fig.12b, has been manufactured with the same procedure used for the wing, and the same materials, i.e., polystyrene, Glass Fabric (GF) and an epoxy resin system (resin + curing agent). The curing cycle was 24 hours at room temperature.

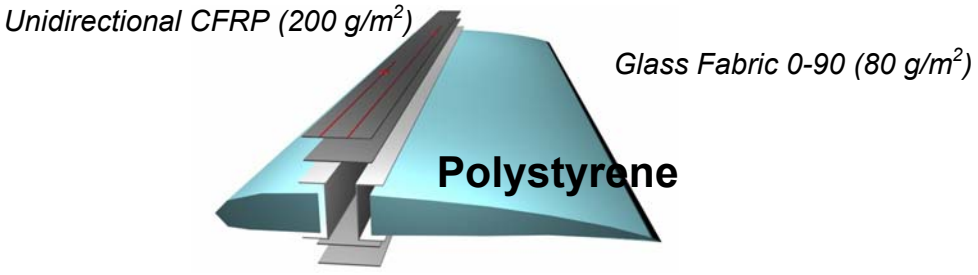

Figure 11: Exploded view of the CFRP spar and the polystyrene body of the wing.

Figure 12a: Photograph of the wing. In white is the body of the wing, in black is the spar.

Figure 12b: Photograph of a detail of the clamped end of the wing.

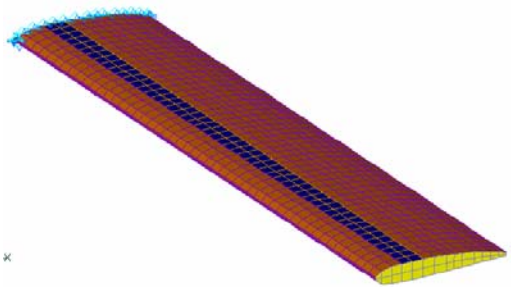

Figure 13: FE model of the wing.

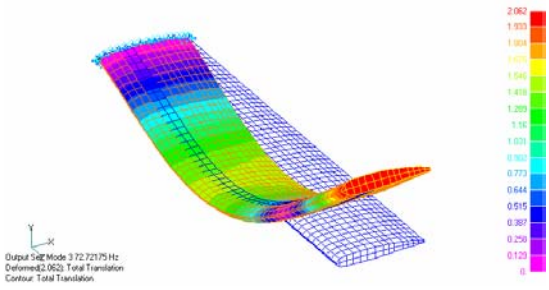

Figure 14: Second finite element bending mode.

Table 1: Natural frequencies of FE model

Frequency	Mode type
10.27	First bending
72.72	Second bending
131.17	First torsional

To reinforce the constraint, two aluminium plates have been glued on the GF. An experimental modal analysis has been performed using for the excitation either an instrumented impact hammer or an electromagnetic shaker. The responses have been measured both with an accelerometer and with the four FBGs embedded in the wing. The electromagnetic shaker has been driven using a stepped sine signal from a signal generator. This type of excitation provides an increased amount of energy to each mode of vibration.

In Fig. 15 is reported as an example the Frequency Response Function (FRF) obtained with the impact hammer and accelerometer, and in Fig. 16 the SFRF relevant to the impact hammer excitation and the fiber optic strain sensor. The response has been obtained using the commercially available Micron Optics

Interrogation System. This system has the limitation in the sampling frequency which is about 50 Hz. Consequently it is not possible to capture mode shapes with natural frequencies above 20Hz. The natural frequencies and the damping coefficients of the FRFs shown in Figs. 15 and 16 are reported in Tab. 2.

Table 2: Experimental modal parameters of First mode shape. Interrogation of FBGs with Micron Optics Instrument.

Frequency	Damping coefficient	Curve fitting	Sensor
$f_1 = 10.47$	$\zeta_1 = 0.024$	YES	Accelerometer
$f_1 = 10.44$	$\zeta_1 = 0.021$	YES	FBG

In Fig. 17a is reported the first strain mode shape as retrieved extracting the modal parameters from the row data of the SFRFs obtained from one of the embedded FBG and in Fig. 17b the corresponding one using the fitted SFRFs . In Fig. 18 are reported the first three mode shapes as retrieved from the FRFs obtained from the accelerometer response and in Tab. 3 the corresponding frequencies and damping coefficients. It can be clearly seen from Fig. 17 and 18a that with both methods the first bending mode of the cantilevered wing does not look exactly as expected. In fact this mode resemble a rigid body motion about the clamped end. Due to the lightweight type of material used it was not possible to tighten the wing end too much. An attempt to model this fact has been performed as mentioned by introducing the spring elements at the constrained end. This also allowed to make a rough adjustment of the first resonant frequencies. The comparison can be performed only on the first two frequencies because with the type of experimental grid chosen (Fig. 12a) only bending modes in the wing span direction could be detected.

Table 3: Experimental modal parameters obtained from accelerometer response.

Frequency	Damping coefficient	Curve fitting	Sensor	Mode type
$f_1 = 10.47$	$\zeta_1 = 0.024$	YES	Accelerometer	First bending
$f_2 = 64.73$	$\zeta_2 = 0.027$	YES	Accelerometer	Second bending
$f_3 = 163.89$	$\zeta_3 = 0.023$	YES	Accelerometer	Third bending

To overcome the limitation imposed by the interrogation system we have also used a home made unit developed at the university of Sannio [42,43]: passive configuration involving broadband interrogation and optical filtering have been used to demodulate returned Bragg signals. Due to the passive nature of the interrogation unit, system bandwidth is only limited by the electronic circuitry involved in the detection unit, actually limited to 400KHz. Consequently with this unit, there were practically no limitations on the interrogation rate. In Fig. 19 are reported the imaginary and the real parts of the SFRFs obtained in the range 0-400 Hz. In Fig. 20 are reported the first and second strain mode shapes obtained from the SFRFs acquired with the high frequency interrogation system. In Tab. 4 are reported the natural frequencies of the first six modes.

In order to have a fully integrated system also the exciting devices should be embedded or surface attached into the structure. The most reliable health monitoring system based on modal parameter estimation is a Multi Input Multi Output (MIMO) system. In an application such as the one at hand, one can think of using two to four piezoelectric patches embedded in different locations on the wing and a much higher number of FBG sensors multiplexed in few optical fibres. To go in this direction, besides the tests described, we have also used a Single Input Multi Output test in which the excitation was given by a shaker B&K 4809 powered by the amplifier B&K 2712 that was driven by a signal generator HP Universal Source 3245. The shaker was connected to the wing tip by a wire. Several stepped sine excitation were applied to the structure, the most accurate being that one centred around the first resonance, i.e., in the range 9-11 Hz with a step of 0.001 Hz every 20 seconds.

Table 4: Experimental natural frequencies obtained with high frequency interrogation system.

Frequency	Curve fitting	Sensor	Mode type
f_1= 9.8	NO	FBG	First bending
f_2= 64.0	NO	FBG	Second bending
f_3 = 45.2	NO	FBG	First torsional
f_4 = 120.0	NO	FBG	Second torsional
f_5= 166.6	NO	FBG	Third bending
f_6=333.3	NO	FBG	Unidentified

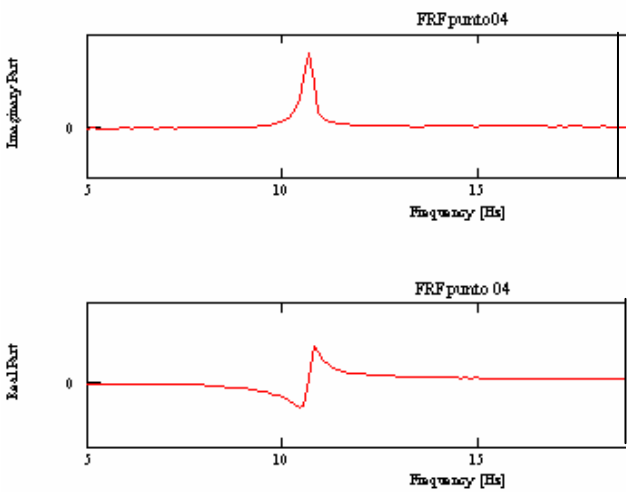

Figure 15: FRF obtained with impact hammer and accelerometer.

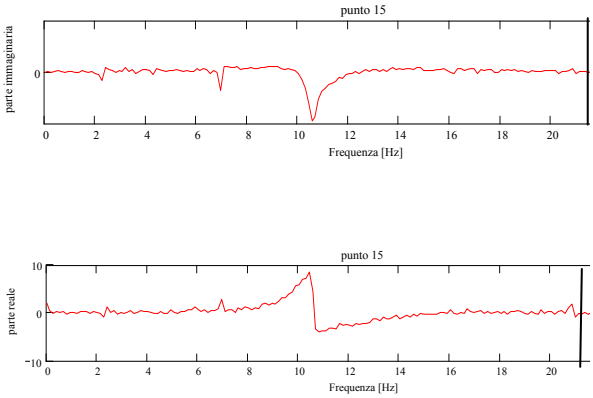

Figure 16: SFRF obtained with impact hammer and FBG.

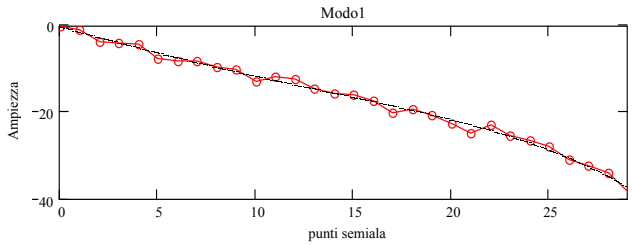

Figure. 17a: First strain mode obtained with unfitted SFRFs of the FBG.

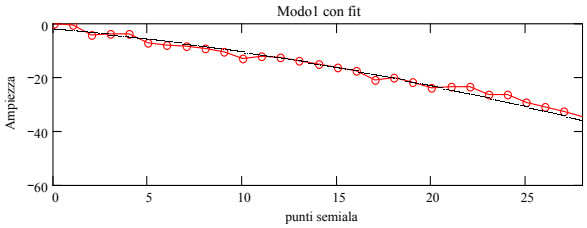

Figure 17b: First strain mode obtained with fitted SFRFs of the FBG.

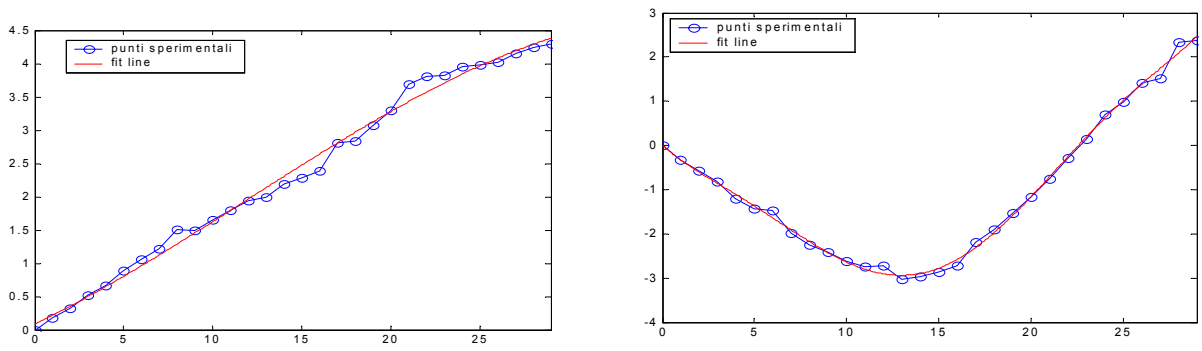

Figure 18: Mode shapes obtained from the accelerometer response.

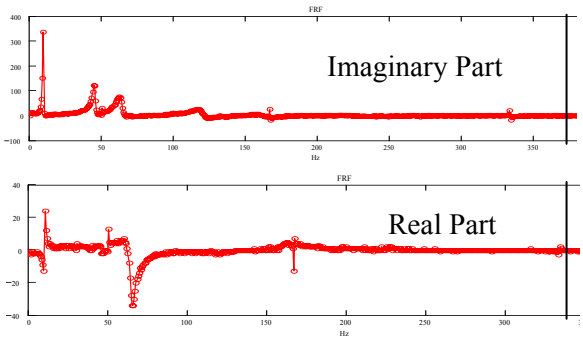

Figure 19: Imaginary and real part of one SFRF relevant to one FBG, obtained with high frequency interrogation system.

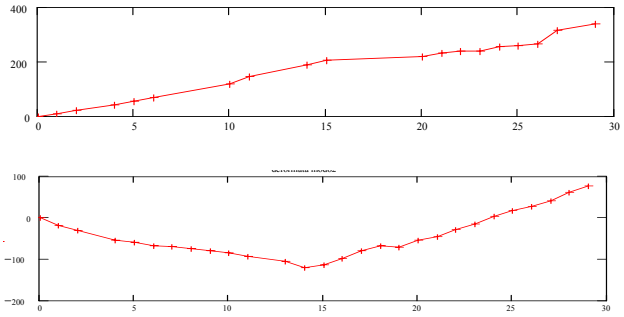

Figure 20: First and second strain mode obtained from the FBG FRFs acquired with the high frequency interrogation system.

3.3 Modal Analysis with Optical Fibres Attached on the Surface of a Metallic Structure

When the SHS system is decided during the design phase of the structure, sensors can be embedded into the materials. Otherwise fibre optic sensors can be glued on existing structures or when the embedding is considered too complicated In Refs. [44,45] for instance the mode shapes of a prototype star tracker using one FBG glued on the external surface of it were determined. In Fig. 21 is reported the test item and the experimental set-up. The thick wires (diameter about 2 mm) are indeed plastic jackets used to protect the optical fibre (diameter 250 μm including the coating). The FBG sensor is inside the fibre and the only way to determine its location while attaching it, is to look at the pencil signs drawn by the FBG manufacturer. Also an accelerometer, for the sake of comparison, has been attached near the FBG. This time the work was not only demonstrative but was useful to check if the prototype was satisfying the structural verification plan requirements which typically impose a minimum value for the first resonant frequency. The Star Tracker under concern is planned for the AMS (Alpha Magnetic Spectrometer) which is a 7 ton particle detector to be mounted on the International Space Station. AMS will provide information on the relative direction (i.e., with respect to itself) and the properties of the particles. The star tracker will provide an inertial reference for AMS and consequently will contribute to determine the location of the particle source in the sky. Once the source is determined, ground and space based observatories can point their instruments to determine further characteristics of the source. In Fig. 23 are reported the first two experimental mode shapes obtained both with the accelerometer (these will be referred to as displacement modes) and the FBG (these will be referred to as strain modes).

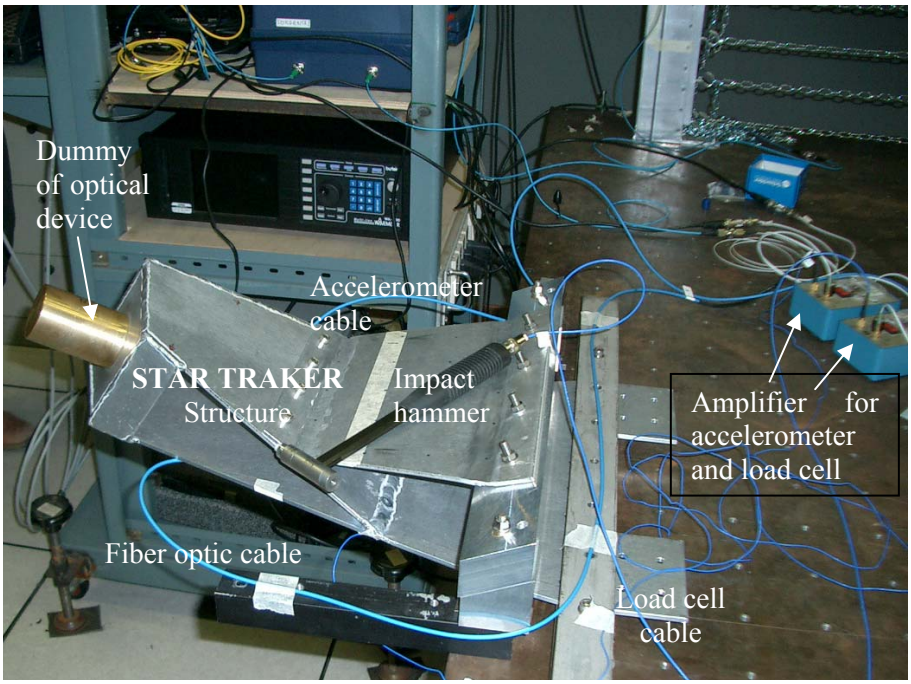

Figure 21: Star tracker prototype with FBG glued on the bottom surface (not visible) and impact hammer for excitation.

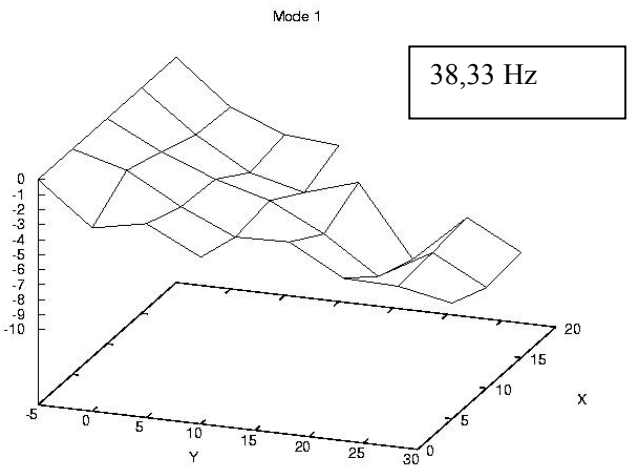

Figure 22a: First experimental displacement mode.

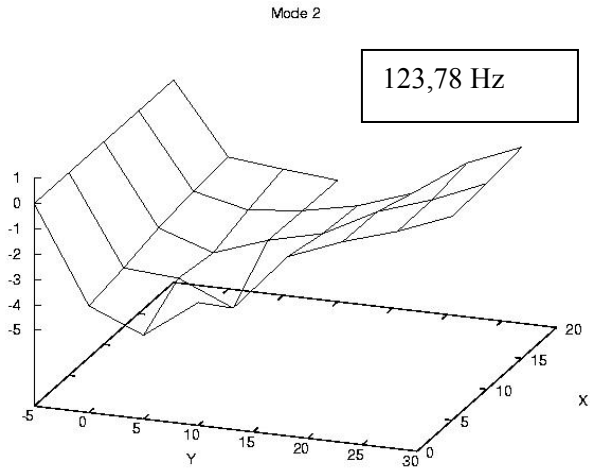

Figure 22b: Second experimental displacement mode.

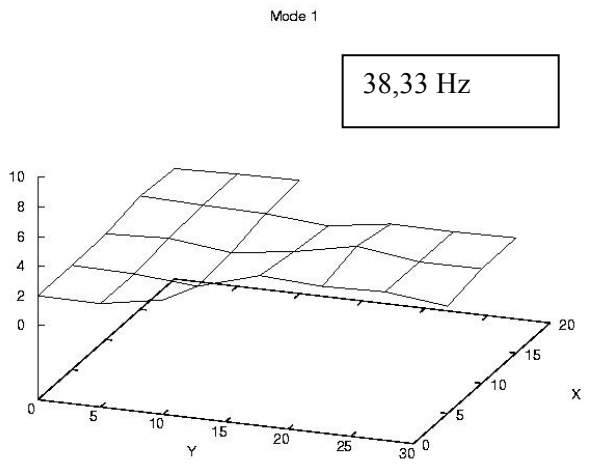

Figure 22c: First experimental strain mode.

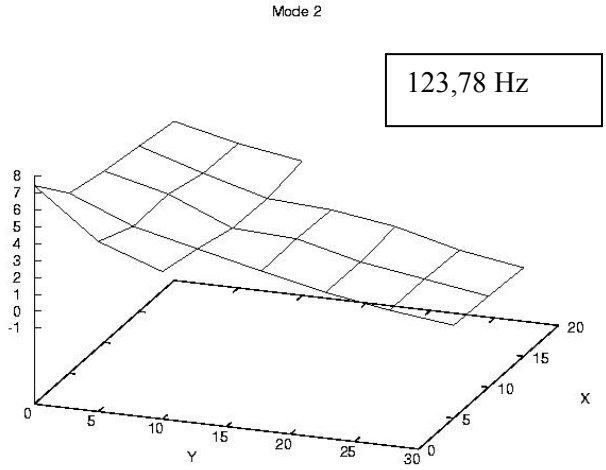

Figure 22d: Second experimental strain mode.

An interpretation of the results reported in Fig. 22 is given hereafter. While the responses of the accelerometer are proportional to the modal displacement or better to their second time derivative, the responses of the FBG at the same frequency are proportional to the strains of the associated modal displacement. Such strains are proportional, for modes that can be essentially considered flexural modes, to the curvature and to the distance from the neutral plane. In other words the strain modes reported in Fig. 22 represent the curvatures of the displacement mode shapes. In fact, taking the second mode as an example, one can clearly see that the curvature of the displacement mode, from the constrained end (left part of figure) toward the tip, decreases continuously starting from the maximum and changing sign toward the end. This behaviour is reflected by the corresponding strain mode.

4 DAMAGE IDENTIFICATION IN TIME DOMAIN

Identification of a damage in a structure from the dynamic responses of the damaged and undamaged structure can be considered as an inverse vibration problem. In fact the direct counterpart of this problem is: given the damaged and undamaged structures find the difference in the responses. Usually inverse problem do not present a unique solution and are generally unstable meaning that even low level of noise can completely spoil the solution. However reformulating the problem as an optimisation procedure it is possible to reduce the problems mentioned above.

Among the inverse problem methods, solved with Variational Approach, the use of the conjugate gradient method [46-48] along with the adjoint equation, has been successfully used for damage identification problems [49-51] In this section we will describe the approach with a numerical example taken from Ref. [52]. The finite element model of a truss space structure has been prepared. A known set of external forces has been applied to the structure in order to provide the time histories of the responses to be used for the stiffness matrix identification and subsequently for damage assessment.

4.1 Finite Element Model of the International Space Station Truss-like Structure

Before to study the effects of the damages on the structure and how to estimate them, an analysis of the dynamic characteristics of the structure (e.g. the natural frequencies and the normal modes) in the undamaged configuration will be presented. Figure 1 shows the layout of the ISS truss-like structure here considered (the number of each element of the finite element model is also reported on the figure), the length of the horizontal and vertical elements is Le = 6 m the total vertical length of the truss is Ly = 42 m,

the maximum width of the truss is Lx = 42 m. In this analysis the structure is clamped on the bottom in order to avoid the rigid motion. The eigenvalues analysis have shown that natural frequencies of the structure span from a minimum value of 2.2 Hz to a maximum value of 450 Hz. In Table 1 the first 15 values of the frequencies are reported.

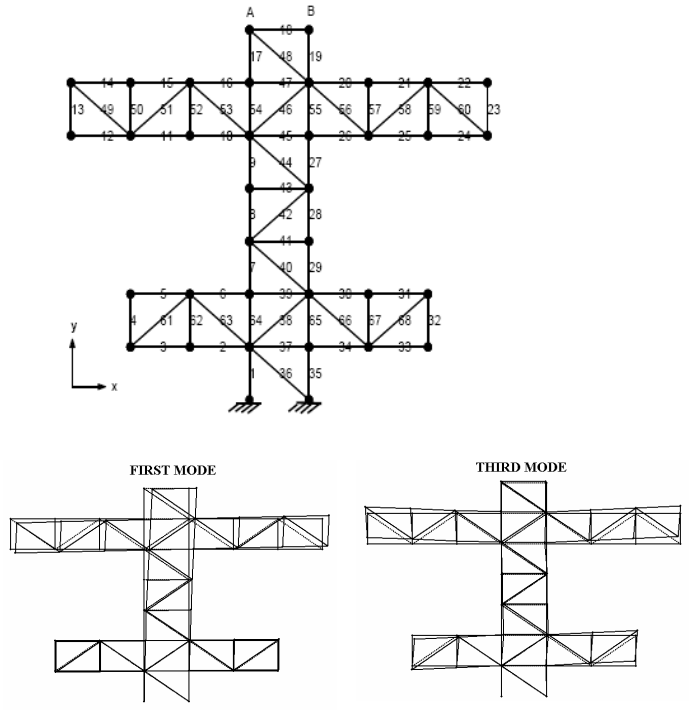

Figure 23: Finite element model.

Nr. of mode	ω (Hz)
1	2.24
2	6.90
3	12.66
4	14.48
5	18.43
6	26.38
7	28.64
8	40.24
9	48.49
10	50.61
11	62.19
12	62.55
13	72.27
14	74.07
15	83.88

Table 5: Natural frequencies of the undamaged structure.

4.2 The Inverse Approach Analysis

The solution of this inverse problem through the Conjugate Gradient Method (CGM) with the adjoint equation involves the steps described in the next subsections.

4.2.1 The Direct Problem

The direct model is given by

$$\mathbf{M}\,\ddot{\mathbf{x}}(t) + \mathbf{C}(t)\,\dot{\mathbf{x}}(t) + \mathbf{K}(t)\,\mathbf{x}(t) = \mathbf{f}(t)\,, \quad t > 0, \qquad \mathbf{x}(0) = \mathbf{x}_0 \quad \text{and} \quad \dot{\mathbf{x}}(0) = \mathbf{y}(0) = \mathbf{y}_0 \tag{1}$$

Where **M** represents the system mass matrix, **K** the stiffness matrix, **C** the damping matrix, **f**(t) the external forces vector, and **x**(t) the displacement vector.

This problem calculates the system displacement vector **x**(t).

4.2.2 The Sensitivity Problem

The inverse problem involves N unknown stiffness parameters, being N the number of elements of the finite element model. The actual parameters in the stiffness matrix are

$$\mathcal{K} = [K_1, \ldots, K_N]$$

and the stiffness matrix is a function of those :

$$\mathbf{K} = f[\mathcal{K}]$$

The N sensitivity problems are obtained by substituting in Eq.1 $\mathbf{K}_j = \mathbf{K}_j + \Delta\mathbf{K}_j$ and $\mathbf{x}_j(t) = \mathbf{x}_j(t) + \Delta\mathbf{x}_j(t)$ (j=1,… N) and by subtracting the resulting expression to Eq. 1:

$$\mathbf{M}\,\Delta\ddot{\mathbf{x}}_j(t) + \mathbf{C}\,\Delta\dot{\mathbf{x}}_j(t) - \mathbf{K}\,\Delta\mathbf{x}_j(t) = \Delta K_j\,\mathbf{x}(t) \quad \Delta\mathbf{x}_j(0) = 0 \quad \text{and} \quad \Delta\dot{\mathbf{x}}_j(0) = 0$$

where the second order terms have been neglected.

4.2.3 The Adjoint Problem

In general, the inverse problem does not satisfy the requirements of existence and uniqueness, then it must be solved as an optimisation problem requiring that the unknown parameter $\mathcal{K}$ should minimize the functional vector defined by:

$$J[\mathcal{K}] = \int_0^{t_f} [\mathbf{x}(t) - \mathbf{x}^{\exp}(t)]^{\mathrm{T}} [\mathbf{x}(t) - \mathbf{x}^{\exp}(t)]\, \mathrm{d}t$$

where t_f is the final time, $\mathbf{x}(t)$ and $\mathbf{x}^{\exp}(t)$ are the computed and measured displacements at time t, respectively. By forming the augmented functional:

$$J[\mathcal{K}] = \int_0^{tf} [\mathbf{x} - \mathbf{x}^{\exp}]^{\mathrm{T}} [\mathbf{x} - \mathbf{x}^{\exp}]\, \mathrm{d}t + \int_0^{tf} \lambda^{\mathrm{T}} \{\mathbf{M}\,\ddot{\mathbf{x}} + \mathbf{C}\,\dot{\mathbf{x}} + \mathbf{K}\,\mathbf{x} - \mathbf{f}\}\, \mathrm{d}t$$

perturbing it, subtracting from the original equation and neglecting the second-order terms, one obtains

$$\Delta J_j[\mathcal{K}] = \int_0^{t_f} 2\,[\mathbf{x} - \mathbf{x}^{\exp}]^{\mathrm{T}} \Delta\mathbf{x}_j\, \mathrm{d}t + \int_0^{t_f} \lambda^{\mathrm{T}} \{\mathbf{M}\,\Delta\ddot{\mathbf{x}}_j + \mathbf{C}\,\Delta\dot{\mathbf{x}}_j + \mathbf{K}\,\Delta\mathbf{x}_j + \Delta K_j\,\mathbf{x}\}\, \mathrm{d}t$$

When the second term of the right-hand side of this expression is integrated by parts and the null initial conditions of the sensitivity problem are employed, the following adjoint problem is obtained for the determination of the Lagrange multiplier vector $\boldsymbol{\lambda}$. The adjoint problem is defined by the following expression with the final conditions on the Lagrange multiplier

$$\mathbf{M}\,\ddot{\boldsymbol{\lambda}}(t) - \mathbf{C}\,\dot{\boldsymbol{\lambda}}(t) + \mathbf{K}\,\boldsymbol{\lambda}(t) = 2[\mathbf{x}^{\exp}(t) - \mathbf{x}(t)] \quad \boldsymbol{\lambda}(t_f) = 0 \quad \text{and} \quad \dot{\boldsymbol{\lambda}}(t_f) = 0$$

4.2.4 The Gradient Equation

During the process for obtaining the adjoint problem, the following integral term was left

$$\Delta J[\mathcal{K}] = \int_0^{t_f} \boldsymbol{\lambda}^{\mathrm{T}} \, \Delta K \, \mathbf{x} \, \mathrm{d}t$$

which is the gradient of the functional ***J***.

4.2.5 The Conjugate Gradient Method of Minimization

The iterative procedure based on the CGM is used for the estimation of the unknown

stiffness parameters $\mathcal{K}$ given in the form

$$\mathcal{K}^{n+1} = \mathcal{K}^n - \beta^n \mathbf{P}^n, \qquad \beta^n = \left\{ \int_0^{t_f} [\Delta \mathbf{x}(t)]^{\mathrm{T}} [\Delta \mathbf{x}(t)] \right\}^{-1} \cdot \left\{ \int_0^{t_f} [\Delta \mathbf{x}(t)]^{\mathrm{T}} [\mathbf{x}(t) - \mathbf{x}(t)^{exp}] \right\}$$

$$n = 0, 1, 2, \ldots,$$

Where [53]:

$$\mathbf{P}^n(t) = J'^n(t) + \gamma^n \mathbf{P}(t)^{n-1}, \quad \text{with} \quad \gamma^0 = 0 \qquad \gamma^n = \frac{\int_0^{t_f} [J'^n(t)]^2 \, dt}{\int_0^{t_f} \left[J'^{n-1}(t)\right]^2 \, dt}, \quad n = 1, 2, \ldots$$

4.3 The Solution Algorithm

The standard computational procedure of the CGM is summarized in the following algorithm:

Step 1: Choose a initial guess $\mathcal{K}^0$ – for example, $\mathcal{K}^0$ = undamaged.

Step 2: Solve the direct problem to obtain x(t).

Step 3: Solve the adjoint problem to obtain $\boldsymbol{\lambda}(t)$.

Step 4: Knowing $\boldsymbol{\lambda}(t)$, compute the gradient function $\mathbf{J}'(\mathcal{K})$.

Step 5: Compute the conjugate coefficient γ^n.

Step 6: Compute the direction of descent $\mathbf{P}^n$.

Step 7: Setting $\Delta\mathbf{K} = \mathbf{P}^n$, solve the sensitivity problem to obtain $\Delta\mathbf{x}(t)$.

Step 8: Compute the step size β^n.

Step 9: Compute $\mathcal{K}^{n+1}$.

Step 10: Test if the stopping criteria is satisfied. If not, go to Step 2.

4.4 Numerical Results

In the following some numerical results will be presented. Two different cases: noiseless and noisy experimental data have been considered. The experimental data have been simulated from the exact solution of the direct problem (noiseless data) or by adding a random perturbation error to the exact solution of the direct problem (noisy data).

The adopted damage scenarios are presented in Table 6 and in order to assess the quality of the estimations the Damage Factor was defined as

$$DF_i = \frac{K_i^u - K_i^d}{K_i^u} \quad i = 1, \ldots, N$$

Table 6: Ten damaged elements and stiffness reduction.

Element	8, 24, 46, 68	4, 29, 52	15, 32, 58
% Reduction	5%	10%	15%

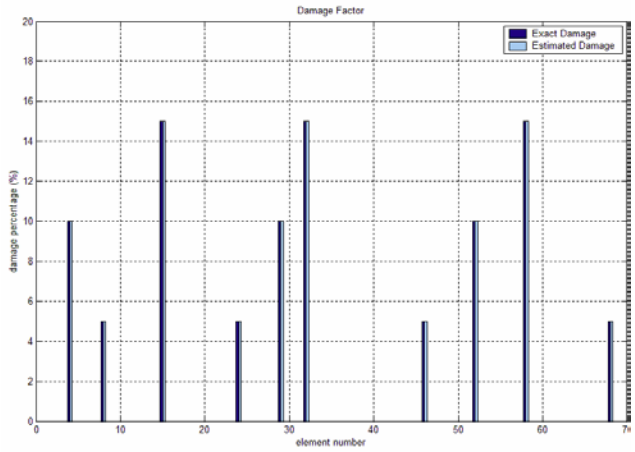

Figure 24: Ten damaged elements: noiseless experimental data.

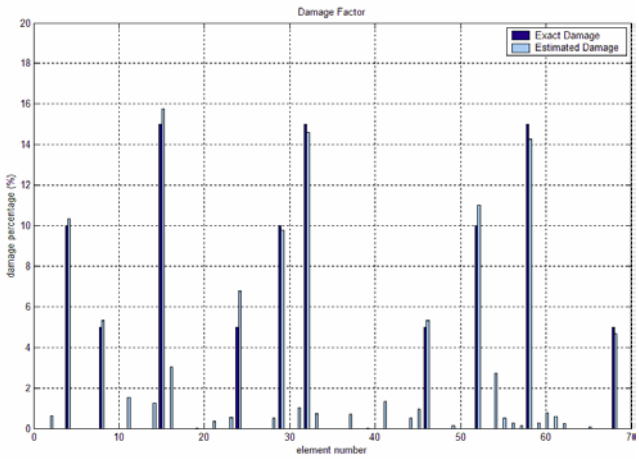

Figure 25: Ten damaged elements: Noisy experimental data.

CONCLUSIONS

After some applications of classical modal analysis techniques, the potential of fibre optic sensors and specifically of the FBG sensors has been shown in practical structures that ranged from composite to metallic ones. In fact those sensors can be used for performing modal analysis both for the purpose of qualification as well as for damage assessment. The sensitivity with respect to damage size it is well known to be limited when modal analysis techniques are used. On the other hand, being a global methodology, it does not require a high number of excitation and sensor points. However fibre optic sensors, differently from accelerometers for instance, provide strain information both statically and dynamically without frequency limitation (frequency limitations are only relevant to the interrogation system). That opens other ways for damage determination such as the one that is currently being investigated that associate ultrasonic wave propagation and FBG sensors. Since Structural Health Monitoring is usually associated with embedding sensors, the investigation of embedding procedures on metallic and polymeric composite materials with fibre optic sensors have been also mentioned. Finally

time domain technique with inverse identification method has been applied numerically on a finite element space structure. The technique can be used with experimental data obtained with FBG sensors. The dynamical tests provided us with natural frequencies and strain mode shapes of different types of structures. However refinements on the embedding process as well as in the data acquisition and analysis are required to favour the wide spread of this technique in practical applications as an alternative or as an integrative technique to conventional non destructing testing.

REFERENCES

[1] Hofer B., "Fiber optic damage detection in composite structures", *Composites*, Vol. 18, No. 4, pp. 309-316, Sept. 1987.

[2] Seo D.C., Lee J.J., "Effect of embedded optical fiber sensors on transverse crack spacing of smart composite structures", *Composite Structures,* Volume: 32, Issue: 1-4, 1995, pp. 51-58.

[3] Paolozzi A., Tempesta G., Ivagnes M., Lecci U., "Behaviour of Aerospace Composite Materials with Embedded Optical Fibers", *PACAM VI/DINAME 99, Applied Mechanics in the Americas*, Rio de Janero Brasil, Jan 1999, vol. 7, pp. 609-612.

[4] Foedinger, R., Rea, D., Sirkis, J., Troll, J., Grande, R., Vandiver, T.L., "Structural Health Monitoring and Impact Damage Detection for Filament Wound Composite Pressure Vessels", Structural Health Monitoring 2000, Ed. Fu-Kuo Chang, *Proc. of 2nd International Workshop on Structural Health Monitoring*, Stanford (CA), pp. 159-169, Sept. 1999.

[5] Paolozzi A., Ivagnes M., Lecci U., "Qualification Tests of Aerospace Composite Materials with Embedded Optical Fibers", *Structural Health Monitoring 2000, Proc. 2nd IWSHM*, Stanford, Sept. 1999 (pp. 661-671).

[6] Paolozzi A., Caponero M.A., Cassese F., Leonardi M., "Use of Embedded Optical fibers for Structural Analysis", *XVII International Modal Analysis Conference (IMAC)*, Orlando, FL, Feb. 1999. (vol. 1, pp. 699-704).

[7] Takeda Nobuo, Characterization of microscopic damage in composite laminates and real-time monitoring by embedded optical fiber sensors, *International Journal of Fatigue,* Volume: 24, Issue: 2-4, February - April, 2002, pp. 281-289.

[8] Asanuma H., Ichikawa K., Kishi T., "Health Monitoring of a Continuous Fiber Reinforced Aluminum Composite with Embedded Optical Fiber", *Journal of Intelligent Material System and Structures*, Vol. 7, pp. 301-311, 1996.

[9] Haga O., Asanuma H., Koyama H., "Mechanical and optical properties of optical fiber embedded super hybrid material" *Advanced Composite Materials,* Vol. 7, no. 3, pp. 239-248, 1998.

[10] Paolozzi A., Felli F., Brotzu A, "Embedding Optical Fibers into Cast Aluminum Alloys", *PACAM VI/DINAME 99, Applied Mechanics in the Americas*, Rio de Janeiro, Brasil, Jan 1999, vol. 8, pp. 1415-1418.

[11] Paolozzi A., Felli F., Caponero M.A., "Global Temperature Measurements of Aluminum Alloy Specimens with Embedded Optical Fibers", *Structural Health Monitoring 2000, Proc. 2nd IWSHM*, Stanford, Sept. 1999, pp. 257-264.

[12] Felli F., Paolozzi A., Caponero M.A., "Fabrication of Intelligent Aluminum Matrix Composite", *Aluminum Transaction*, vol. 2, pp. 189-194.

[13] Caponero M.A., Felli F., Mazzoni G., Paolozzi A., "Crack growth measurements on a composite specimen using fiber optic sensors", *JSME/ASME International Conference on Materials and Processing 2002 (M&P2002)*, Hawaii, October 15-18, 2002, pp. 406-411.

[14] Seo D.C., Lee J.J., Kwon I.B., "Monitoring of fatigue crack growth of cracked thick aluminum plate repaired with a bonded composite patch using transmission-type extrinsic Fabry–Perot interferometric optical fiber sensors", *Smart Materials and Structures,* Volume: 11, Issue: 6, December 01, 2002, pp. 917-924.

[15] Paolozzi A. (1999), "A space Debris Monitoring System for the ISS Based on Optical fibers", *XV Congresso Nazionale AIDAA*, Torino, Italy, Oct, 1999. pp. 803-810.

[16] Benussi L., Bertani M., Bianco S., Caponero M.A., Fabbri F.L., Felli F., Giardoni M., La Monaca A., Pace E., Pallotta M., Paolozzi A., "Use of Fiber Bragg Grating Sensor for Position Monitoring in High Energy Physics Experiment BTeV", *IEEE Sensor 2002*, Kissimmee, FL, June 2002, (pp. 874-879).

[17] Benussi L., Berardis S., Caponero M.A., Colonna D., Felli F., Paolozzi A., et al. (2003), "Fiber Optic Sensors for Space Missions", *IEEE Aerospace Conference*, Montana, Big Sky, March 8-15, 2003.

[18] Caponero M.A., Felli F., Paolozzi A., "Vibration Tests on Metal Alloys with Embedded Optical Fibers", *SPIE's Symposium on smart Materials and MEMS (Smart Material),* Melbourne, Australia, Dec.13-15, 2000, vol. 4234, pp. 152-159.

[19] Paolozzi A., Felli F., "Broad Band Tests on Metallic Specimens by embedded Optical Fibers", *XVI AIDAA*, Palermo , Sept. 2001, pp. 1-10, paper no. 103.

[20] Caponero M.A., Felli F., Paolozzi A. (2001), "Strain Measurements with FBGs Embedded into Cast Metal Alloys", *7th Japan Int. SAMPE Symp. and Exhibition (JISSE 7)*, Tokyo Nov. 2001, pp. 661-664.

[21] Paolozzi A. (2001), "Recent Researches on Fibre Optic Smart Structures in Italy and Future Trends in Europe", Key note at the *7th Japan Int. SAMPE Symp. and Exhibition (JISSE 7),* Tokyo, Nov. 2001, pp. 35-42.

[22] Paolozzi, A., Caponero, M.A., Felli, F., Colonna, D., "Vibration tests on a composite cantilever beam by fibre Bragg Gratings", *Proc. of the Intern. Conf. on Structural Dynamics Modelling*, Madeira, Portugal, June, 2002.

[23] Paolozzi A., Caponero M.A., Sarasso M., Colonna D., "Static and Dynamic Measurements on an Aerospace Composite Beam by Embedded Fiber Optic Sensors", *JSME/ASME International Conference on Materials and Processing 2002 (M&P2002)*, Hawaii, October 15-18, 2002, pp.384-389.

[24] C.M. Vest, "Holographic Interferometry", John Wiley & Sons, New York, 1979.

[25] M.A. Caponero, A. Paolozzi, I. Peroni, R. Rizzo, "Mode Shape Experimental Holographic Technique for Spacecraft Sandwich Panels", Proceedings 14th International Modal Analysis Conference (IMAC), pp. 1539-1545, Dearborn, Michigan, Feb. 1996.

[26] M.A. Caponero, A. Paolozzi, I. Peroni, "Modal Tests on the Full-scale Model of a Microsatellite", 15th International Modal Analysis Conference (IMAC), pp. 470-475, Orlando, Florida, Feb. 1997.

[27] M.A. Caponero, A. Paolozzi, P. Pasqua, I. Peroni, "Use of Holographic Interferometry and Electronic Speckle Pattern Interferometry for Measurement of Dynamic Displacements", Mechanical Systems and Sygnal Processing, Vol. 14, N. 1, pp. 49-62, Jan. 2000.

[28] R. Jones, C. Wykes, "Holographic and speckle interferometry", 2nd ed. Cambridge, UK: Cambridge University Press, 1989.

[29] M.A. Caponero, G.B. Palmerini, A. Paolozzi, I. Peroni, "Influence of the Constraints on the Modal Parameters of a Microsatellite", Atti del XV Congresso Nazionale AIDAA, Torino, Italy, pp. 1245-1256, Ott, 1999.

[30] M.A. Caponero, A. Paolozzi, P. Pasqua, I. Peroni, "Modal Pattern Detection of Aerospace Sandwich Structures by Speckle Interferometry", 16th International Modal Analysis Conference (IMAC), Santa Barbara, CA, pp. 1257-1263, Feb 1998.

[31] A. Agneni, M.A. Caponero, A. Paolozzi, "Image processing for Fringe Unwrapping in Speckle Interferometry" Proc. XVIII International Modal Analysis Conference (IMAC), S. Antonio, TX, pp. 1479-1484, Feb. 2000.

[32] M.A. Caponero, A. Paolozzi, I. Peroni, "Use of Speckle Interferometry and Modal Assurance Criterion for Identification of Component Modes", Optics and Lasers in Engineering (**37**), pp. 355-367, 2002.

[33] L. Balis Crema, A. Castellani, A. Paolozzi, I. Peroni, "Identificazione Mediante Analisi Sperimentale di un Modello Dinamico di una Pala per Aerogeneratore", Atti VIII Congresso Nazionale AIDAA, Torino, pp. 507-523, Sept. 1985.

[34] I. Peroni, A. Paolozzi, A. Bramante, "Modal Analysis on a Model of the Italsat Satellite", Proceedings 9th International Modal Analysis Conference, pp. 1574-1582, 1991.

[35] J. Crowley, E. Peterson, R. Russel, "Multiple-input method speeds space shuttle testing", Sound and Vibration, pp. 13-20, June 1983.

[36] G. D. Carbon, D.L. Brown, R.J. Allemang, "Application of dual input excitation techniques to the modal testing of a commercial aircraft", 1st IMAC Proceeding, pp. 539-565, 1982.

[37] O. Bernasconi, D.J. Ewins, "Application of Strain Modal Testing to Real Structures", 6th International Modal Analysis Conference, Vol. 2, pp.1453-1464, 1988.

[38] A. Paolozzi, I. Peroni, "Detection of Debonding Damage in a Composite Plate Through Natural Frequency Variations", Journal of Reinforced Plastics and Composites, Vol. 9, pp. 369-389, July 1990.

[39] I. Peroni, A. Paolozzi, A. Bramante, ``Effect of Debonding Damage on the Modal Damping of a Sandwich Panel'', Proceedings 9th International Modal Analysis Conference, pp. 1617-1622, 1991.

[40] A. Agneni, A. Paolozzi, I. Peroni, "Damage Detection by Modal Parameter Estimation", Aerotecnica Missili e Spazio, Vol. 70, n. 3-4, pp. 141-146, 1991.

[41] A. Paolozzi, I. Peroni, "Experimental assessment of debonding damage in a carbon-fiber reinforced plastic sandwich panel by frequency variation", Composite Structures, 35 (4), pp. 435-444, 1996.

[42] Cusano A., Breglio G., Cutolo A., Calabrò A., Giordano M., Nicolais L., "All Fiber Bragg Grating Sensing System for Static and Dynamic Strain Measurements", *Proc. of the Third International*

conference on Structural Health Monitoring, Stanford University, September 10-12, 2001, pp. 1158-1164.

[43] Cusano A., Persiano G.V., Breglio G., Nasser J., Giordano M. "Dynamic Strain Measurements by Fibre Bragg Grating Sensor", *Eurosensors XVI Conference*, Prague, September 2002 pp. 345-349.

[44] M.A. Caponero, D. Colonna, A. Cusano, C. Gargiulo, A. Paolozzi, I. Peroni, "Dynamic Measurements on a Star Tracker Prototipe of AMS Using Fiber Optic Sensors", XVII AIDAA Congress, pp. 1685-1695 Roma, 15-19 Sept. 2003.

[45] A. Cusano, P. Capoluongo, S. Campopiano, A Cutolo, M. Giordano, M.A. Caponero, F. Felli, A. Paolozzi, "Dynamic Measurements on a Star Tracker Prototipe of AMS Using Fiber Optic Sensors", Smart Material Structures, Vol. 15, pp. 441-450, 2006. (Upgraded version of ref. [44].

[46] O.M. Alifanov, Solution of an inverse problem of heat conduction by iteration methods, J. Eng. Phys., 26(4) (1974) 471-476.

[47] L.D. Chiwiacowsky, H.F. Campos Velho, Different Approaches for the Solution of a Backward Heat Conduction Problem, Inverse Probl. Eng., 11(6) (2003) 471-494.

[48] L.D. Chiwiacowsky, H F. de Campos Velho, P.Gasbarri, The Damage Identification Problem: an Hybrid Approach , 2nd Thematic Congress onDynamics and Control (DINCON 2003), 18-22 August, Sao Jose dos Campos (SP),BRAZIL, 1393-1402 - ISBN 85-86883-15-8.

[49] L.D. Chiwiacowsky, H F. de Campos Velho, P.Gasbarri, Determining Stiffness Matrix by the Adjoint Method, International Conference on Computational & Experimental Engineering and Sciences, Madeira, Portugal, 26-29 Luglio, 2004.

[50] Chiwiacowsky, L. D. ; Velho, Haroldo Fraga de Campos ; Gasbarri , P . A Solution for the Damage Assessment Problem by the Adjoint Equation Method. XXVII Congresso Nacional de Matemáca Aplicada e Computacional, 2004, Porto Alegre, 2004.

[51] Velho, Haroldo Fraga de Campos; Chiwiacowsky, L. D.; Gasbarri, P. ; Some Results on Damage Detection Using Variational Approach . In: 4th Thematic Congress on Dynamics and Control (DINCON), Bauru, 2005.

[52] Chiwiacowsky, L. D. ; Gasbarri, Paolo ; Velho, Haroldo Fraga de Campos . Damage Assessment of Large Space Structures Through the Variational Approach ,International Astronautical Congrss IAC-2004 & Vancouver Canada, 1-8 Oct.2004.

[53] Chiwiacowsky, L. D.; Velho, Haroldo Fraga de Campos ; Gasbarri, P. A Variational Approach for Solving an Inverse Vibration Problem , Inverse Problem in Sciences and Engineering, Vol. 14, No.5 July 2006, pp.557-577.

SYMPOSIA DISCUSSION – PAPER NO: 9

Author's Name: A. Paolozzi

Question (W. Baron):
How was the FBG used on the small UAV? What support equipment is needed?

Author's Response:
Four FBG were embedded into the CFRP composite spar and GRP skin. The measurements were performed only on the ground, with two different equipments, called FBG interrogation systems. These interr. systems needed to be connected to a portable computer for data acquisition. The weight of P.C. + Interrogation system was between 3 to 6 kg, compatible with UAV performance, and they could have been used for real time data acquisition in flight.
However UAV was developed for a competition and risk of crash was not negligible. We performed only ground test (modal analysis) in which excitation (with impact hammer) was known. One interr. system was high frequency (i.e. could read thousands of time per second the FBG strain) but with lower accuracy; the other one had an accuracy of 1 microstrain and an interr. frequency of 50 Hz. With this system only it was possible to detect the first mode.